A Journal of the Gesellschaft Deutscher Chemiker
Angewandte
GDCh
International Edition
Chemie
www.angewandte.org

# Accepted Article

**Title:** Hydrogen Bonding Regulated Supramolecular Nanostructures and Impact on Multivalent Binding

**Authors:** Suhrit Ghosh, Amrita Sikder, Debes Ray, and Vinod K Aswal



**To be cited as:** *Angew. Chem. Int. Ed.* 10.1002/anie.201812217
*Angew. Chem.* 10.1002/ange.201812217

**Link to VoR:** http://dx.doi.org/10.1002/anie.201812217
http://dx.doi.org/10.1002/ange.201812217

WILEY-VCH

10.1002/anie.201812217


WILEY-VCH

# Hydrogen Bonding Regulated Supramolecular Nanostructures and Impact on Multivalent Binding

Amrita Sikder[a], Debes Ray[b], Vinod K Aswal, [b] and Suhrit Ghosh*[a]

**Abstract:** This communication reveals H-bonding regulated nanostructure, thermodynamics and multivalent binding of two bola-amphiphiles (NDI-1, NDI-2) consisting of a hydrophobic naphthalene-diimide (NDI), connected to a hydrophilic wedge by a H-bonding group and a glucose moiety on its two arms. They differ by the single H-bonding group, namely hydrazide and amide, which triggers formation of vesicle and cylindrical micelle, respectively. H-bonding among the rigid hydrazides in NDI-1 contributes to a major enthalpy gain and relatively less entropy gain. For NDI-2, a relatively less enthalpy gain is compensated by the additional entropy originated from the conformational freedom of the open structure. Although the extended H-bonding ensures stacking with head-to-head orientation and multiple array of the appended glucose moieties in both systems, adaptive cylindrical structure exhibits superior multivalent binding with Concanavalin (ConA) than that of the vesicle. Control amphiphile (NDI-3), lacking any H-bonding group, assembles with random lateral orientation, producing spherical micelle without any notable multivalent binding.

Aggregation of amphiphilic molecules [1] and macromolecules [2] produce wide ranging nanostructures depending on the structure of the unimer. Surface functional group display in these nanostructures endows multivalent binding [3] with cell surface,[4] protein,[5] DNA,[6] heparin[7] and other biological targets which has important applications. To achieve effective and specific multivalent binding in the complex biological milieu, it requires precise engineering of these nanostructures by taking into consideration of several issues such as stability, morphology, surface functional group display and density, adaptability and so on. In this regard, supramolecular polymers of π-systems in water [8, 9] appear promising owing to their precise internal order, stability, optical properties and the possibility to fine tune the structural parameters by directional molecular interaction unlike the immiscibility driven aggregation of classical amphiphiles. We have recently developed [10] a supramolecular strategy that enables H-bonding regulated unidirectional assembly of a bola-shape π-amphiphile (NDI-1a, Scheme 1) and construction of unsymmetric vesicle. The propensity of the H-bonded chain of the hydrazides to remain shielded at the inner wall prevailed over electrostatic and/or steric factors resulting in display of the anionic groups at the outer surface. To test the scope of this design for synthesis of precision nanostructures with desired functional group display and multivalent binding with biological targets, we have studied a few new NDI-derived unsymmetric bola-amphiphiles (Scheme 1). NDI-1 and NDI-2 differ merely by the H-bonding group, hydrazide and amide, respectively, while NDI-3 lacks any H-bonding functionality. All of them contain a glucose so that the impact of the supramolecular assembly on multivalent binding can be studied using Lectin as the model biological target. [11] This communication reveals the remarkable impact of a marginal structural difference in the unimer on the morphology, thermodynamics and multivalent binding ability of the resulting nanostructures.

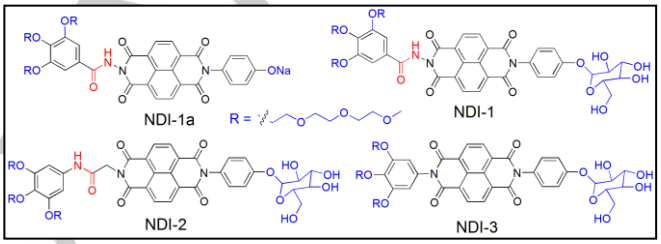


**Scheme 1.** Structure of various NDI-amphiphiles

Dynamic light scattering (DLS) of NDI-1 showed a sharp peak with average $D_h$ of ~160 nm while that for NDI-2 indicated much larger aggregates (Fig 1a). Transmission electron microscopy (TEM) images (Fig 1b, S1) showed hollow spherical structures for NDI-1 with diameter in the range of 150-200 nm corroborating with the DLS. UV/Vis spectra (Fig S2) of Calcein treated NDI-1 aggregates revealed 13 % dye loading efficiency which matches with reported values for vesicles of comparable size.[12] Absorption normalized florescence intensity of the entrapped Calcein was found to be significantly less (Fig S2) compared to that of the free dye in water, which typically has been attributed to self-quenching of the dye in the water filled lacuna of vesicles.[13] These observations corroborate with our previous reports[10] in supporting vesicular assembly of NDI-1. In sharp contrast, TEM image of NDI-2 (Fig 1c, S1) showed 1D fibrils with diameter of ~ 25-30 nm and length extending over a few micrometers. [14-15] Differing with both, NDI-3 formed relatively smaller spherical particles (Fig 1d, S1) with diameter in the range of 40-60 nm which was consistent with DLS (Fig 1a) revealing $D_h$ of 50-60 nm. To further elucidate the morphological differences, small-angle neutron scattering (SANS) experiments were performed (Fig 2). [16] The SANS data from NDI-1 was analyzed using a model of unilamellar vesicles (ULV). In the low-$Q$ region (< 0.05 Å$^{-1}$), the scattering intensity decreased in a straight line as $1/Q^2$ indicating presence of large vesicles. At higher $Q$ values (> 0.05 Å$^{-1}$), there was increase in the drop of the intensity and a minimum was observed, which depends on the thickness of the hydrophobic component (monolayer). These ULVs thus were characterized by the monolayer thickness ($t$) = 12.1±0.7 Å as the measurement of the radius of the vesicle ($R_v$) was limited by the $Q_{min}$ of the SANS instrument.

[a] Ms Amrita Sikder and Professor Dr. Suhrit Ghosh
School of Applied and Interdisciplinary Sciences, Indian Association for the Cultivation of Science, Kolkata, India-700032
E-mail: psusg2@iacs.res.in
[b] Dr. Debes Ray and Dr. Vinod K Aswal
Solid State Physics Division, Bhabha Atomic Research Centre, Mumbai-400085
E-mail: vkaswal@barc.gov.in

Supporting information for this article is given via a link at the end of the document.

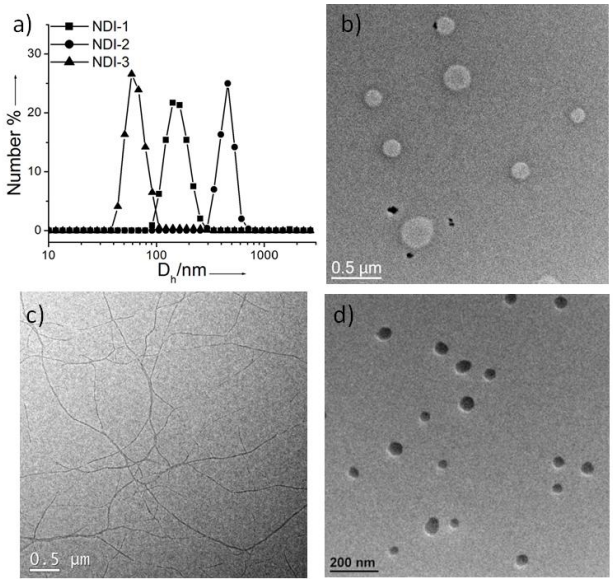


**Fig 1.** a) Particle size distribution of different aggregates obtained from DLS; TEM images of nanostructures obtained from aqueous solution of b) NDI-1, c) NDI-2 and d) NDI-3. *C* = 1.0 mM. Black spots in b) could be drying artifacts.

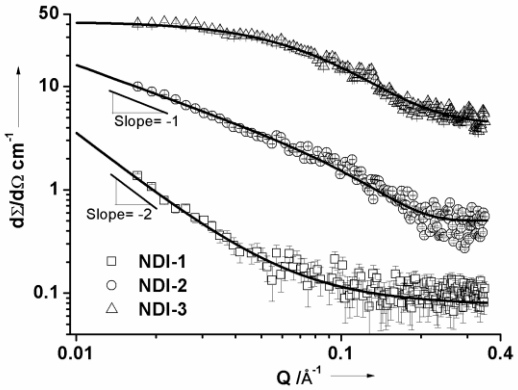


**Fig 2.** SANS plot of the scattering intensity as a function of scattering vector Q for NDI-amphiphiles. The plots for NDI-2 and NDI-3 are vertically shifted for clarity.

The absence of lower cut-offs in the data indicates that the radii of the vesicles could be larger than what could be determined from the present $Q_{min}$ and therefore the radius of the vesicle was kept fixed at a higher value than to a value of $2\pi/Q_{min}$, i.e., ~350 Å. The inaccessibility of the SANS data at low-*Q* has been addressed with the use of static light scattering (SLS) technique. From SLS, using Guinier approximation (Fig S3), the radius of the vesicles was found to be ~72 nm which is in close agreement with the hydrodynamic radius $R_h$ (~ 75 nm) obtained from DLS.The SANS data of NDI-2 was distinctly different and analyzed using a model of long cylinders. In the low-*Q* region of the data, the scattering intensity decreased following a power law as 1/*Q* indicating the formation of long cylindrical micelles. These cylinders were characterized by the cross-sectional radius ($R_{cr}$) = 13.2±0.8 Å while the measurement of their length (*L*) was limited by the $Q_{min}$ of the instrument. Noteworthy that the diameter of the fibers was estimated to be 25-30 nm from TEM image (Fig 2c). The difference can be attributed to the lateral clustering of the individual fibers in the dry state TEM while SANS could probe the diameter of the single fiber. On the other hand, NDI-3 was found to consist of spherical micelles with core radius ($R_c$) = 11.8±0.7 Å and the polydispersity ($\sigma$) = 0.22±0.03. Thermodynamic parameters associated with aggregation were estimated (Table 1) from the isothermal titration calorimetry (ITC). [17] Fig 3 shows an ITC dilution experiment of NDI-1 revealing an endothermic heat flow which saturated beyond a certain concentration. The experiment was repeated for two more times (Fig S4) while consistent results were obtained. The initial heat change was assigned to the heat of dissociation while beyond the saturation only the heat of dilution persisted. Likewise ITC experiments were performed for NDI-2 and NDI-3 (each in triplicate) which revealed similar trends (Fig S5, S6).The saturation concentration was considered as the critical aggregation concentration (CAC) while the difference of heat between the initial and final state was taken as the enthalpy of aggregation ($\Delta H$). For NDI-1, concentration dependent UV/Vis studies (Fig S7) revealed a CAC value of 0.17 mM which corroborated with the ITC estimated value (Table 1). The free energy ($\Delta G$) and the entropy ($\Delta S$) of aggregation were estimated using these ITC data following reported procedure (see SI for detail). $\Delta H$ and CAC varied in the order NDI-1 > NDI-2 > NDI-3 and NDI-1 < NDI-2 < NDI-3, respectively, which is attributed to a relatively stronger H-bonding between hydrazides than amides [15] and lack of H-bonding in NDI-3.

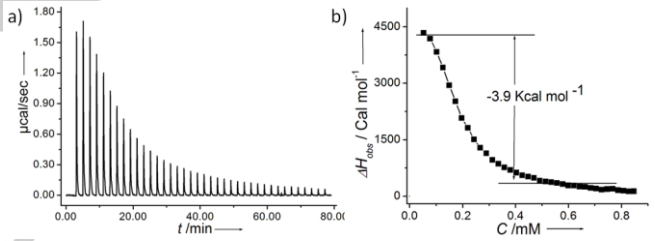


**Fig 3.** a) Heat release per injection of an aqueous solution of **NDI-1** in ITC dilution experiment (C=5.0 mM, T= 25 °C) and b) corresponding enthalpogram.

**Table 1.** Thermodynamic parameters (average values have been reported from three independent ITC experiments) associated with the aggregation of various NDI derivatives.

| System | CAC (mM) | $\Delta H$ ($kCalM^{-1}$) | $\Delta S$ ($CalM^{-1}K^{-1}$) | $\Delta G$ ($kCalM^{-1}$) |
|---|---|---|---|---|
| NDI-1 | 0.15±0.02 | - 3.9±0.04 | 4.4±0.1 | -5.2±0.04 |
| NDI-2 | 0.29±0.03 | -0.65±0.05 | 13.2±0.1 | -4.8±0.05 |
| ND- 3 | 0.4±0.05 | -0.4±0.04 | 13.9 ±0.3 | -4.5±0.07 |

FT-IR spectra (Fig S8) of NDI-1 in THF showed a distinct peak at 1702 $cm^{-1}$ assigned to the CO stretching of the non-bonded hydrazide which shifted to 1672 $cm^{-1}$ in $D_2O$ and also in bulk suggesting H-bonding. For NDI-2, the amide carbonyl stretching peak merged with the imide carbonyl peaks of NDI and thus quantitative analysis was not possible. However, by comparing the spectra in THF, $D_2O$ and bulk (Fig S9), H-bonding among the amide groups was evident in $D_2O$. Positive $\Delta S$ values indicated entropically favourable supramolecular assembly in all

three systems [18] and attributed to the hydrophobic effect [8c, 19] due to the release of the surrounding water molecules during aggregation. Nevertheless, significantly higher $\Delta S$ values estimated for NDI-2 and NDI-3 compared to NDI-1 cannot be rationalized only by the hydrophobic effect as the π-surface remains the same in all three systems. Possibly, 1D fibrils of NDI-2 enjoys more conformational freedom than vesicles of NDI-1 and therefore the former is entropically more favourable. On the other hand, lack of any H-bonding induced restriction makes the NDI-3 aggregates more disordered and dynamic which contributed to the enhanced entropy. It is noteworthy that by enthalpy-entropy compensation, the ΔG values appear to be comparable for all the three systems.

We examined the impact of supramolecular structure on the binding affinity with a lectin protein ConcanavalinA (ConA) which specifically binds with α-D-mannosyl and α-D-glucosyl ligands.[11] When aqueous solutions of NDI-1 or NDI-2 were treated with ConA, the mixture instantly became turbid (Fig 4) indicating efficient glycocluster effect. In sharp contrast, a mixture of ConA and NDI-3 did not produce much turbidy suggesting lack of efficient binding. Optical density (at 420 nm) as a function of time showed a sharp rise for both NDI-1 and NDI-2 up to first 2 minutes after mixing followed by saturation indicating fast binding. Higher optical density in case of NDI-2 than NDI-1 may suggest enhanced glycoclustering in presence of the linear supramoleular structure. To estimate the binding affinities, fluorescence quenching titration was performed using fluorescein isothiocyanate tagged ConA (FITC-ConA). Fluorescence intensity of FITC-ConA decreased by ~ 80 % upon gradual addition of NDI-1 (Fig 4)[20] and from these data $K_a$ was estimated to be $3.2\times10^3$ $M^{-1}$ using the Steck-Wallack plot [21] (Fig 4d) which is in the similar range with polymeric nanostructures.[11] In sharp contrast, negligible florescence change was noticed (Fig S10) for NDI-3 which suggested lack of any multi-valent binding.[22] When similar experiment was performed with NDI-2 (Fig S11), the $K_a$ ($1.35\times10^4$ $M^{-1}$) was found to be almost an order of magnitude higher than NDI-1 suggesting cylindrical structure to have even superior impact than vesicular structure for multivalent binding.

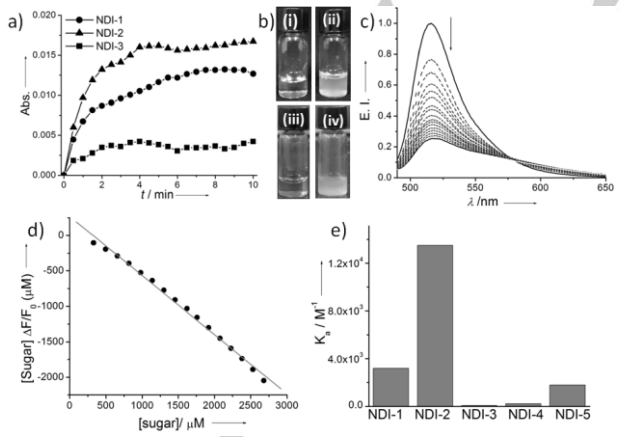


**Fig 4.** a) Variation of absorbance at 420 nm as a result of scattering in the mixture of Con A and NDI-derivatives (C=1.0 mM); b) Picture of aqueous dispersions of (i) NDI-1 (ii) NDI-1+ConA (iii) NDI-2 and (iii) and (iv) NDI-2+ConA (C=1.0 mM); c) Change in fluorescence intensity of FITC ConA with gradual addition of NDI-1(C=0.1 mg/mL, $\lambda_{max}$= 480 nm); d) Steck- Wallack plot of fluorescence intensity change in FITC-ConA with NDI-1; e) Relative $K_a$ values for binding of ConA with various NDI derivatives (Scheme 1 or 2).

A model to rationalize the observed variations has been proposed in Scheme 2. Involvement of H-bonding among the hydrazides in the π-stacked assembly of NDI-1 ensures a fixed uni-lateral orientation of leading to the formation of unsymmetric vesicles. Excellent binding efficiency with ConA confirms the display of the glucose moieties in the outer surface of the vesicle which is consistent with our earlier report. [10] In our earlier report, [10] it was shown that the functional group display depends on the location of the hydrazide group as the direction of the curvature was determined by the preference of the H-bonded chain to remain at the inner wall of the vesicle. To verify whether a similar control exists in the present system, NDI-4 (Scheme 2) was studied which differs with NDI-1 merely by the location of the hydrazide group. UV/Vis and DLS experiments (Fig S12) confirmed aqueous aggregates of NDI-4. However, unlike NDI-1, in this case no glycocluster effect was noticed (Fig S13). Binding study with FITC-ConA revealed (Fig S14) negligible change in the fluorescence intensity indicating lack of multi-valent binding. Such sharp contrast between NDI-1 and NDI-4 ascertains that the surface display of the sugar units is regulated solely by the location of the hydrazide group. To further examine whether all the glucose moieties in NDI-1 were displayed at the outer wall, its binding affinity was compared with NDI-5 (Scheme 2), having sugar moieties in both ends. It also showed signature of aggregation in water as evident from UV/ Vis and DLS (Fig S15). In this case $K_a$ was estimated to be $1.7\times10^3$ $M^{-1}$ from fluorescence studies (Fig S16). The fact that $K_a$ for NDI-1 is even higher than that of NDI-5 strongly favors the hypothesis on uni-directional orientation of NDI-1 in vesicular assembly (Scheme 2). Slightly lower value for NDI-5 may be related to its restricted mobility due to the presence of two hydrazide groups. On the other hand, NDI-3, lacking any H-bonding restriction, stacks with irregular lateral orientation leading to the micellar structure with random distribution of the oligo-oxyethylene wedge and the sugar groups on the surface resulting in negligible glycocluster effect. Lack of accessibility of the ligand due to crowding might have also inhibited efficient interaction. Interesting is the comparison between NDI-1 and NDI-2. A mere difference in the nature of the H-bonding group appears to make a sea change in the morphology which can be attributed to the difference in internal order of the molecular assembly in these two systems which was evident from their UV/Vis spectra (Fig S17). Firstly, the UV/Vis spectra of all three systems in water indicated π-stacking. [23] But for NDI-2, the spectrum showed a more prominent bathochromic shift (6 nm) and a red-shifted band appeared at 387 nm indicating longitudinal displacement of the chromophores [24] which possibly triggered the formation of elongated 1D structure. In contrast for NDI-1, the distinct H-bonding motif of the hydrazide compelled a face to face stacking and provided the curvature for vesicular structure. Open chain 1D structure of NDI-2 is expected to be more adaptive than NDI-1 vesicle, rendering better glycocluster effect which requires adjustment of the conformation of the multi-valent ligand to simultaneously binds to the four binding centers of the tetrameric ConA.[11]

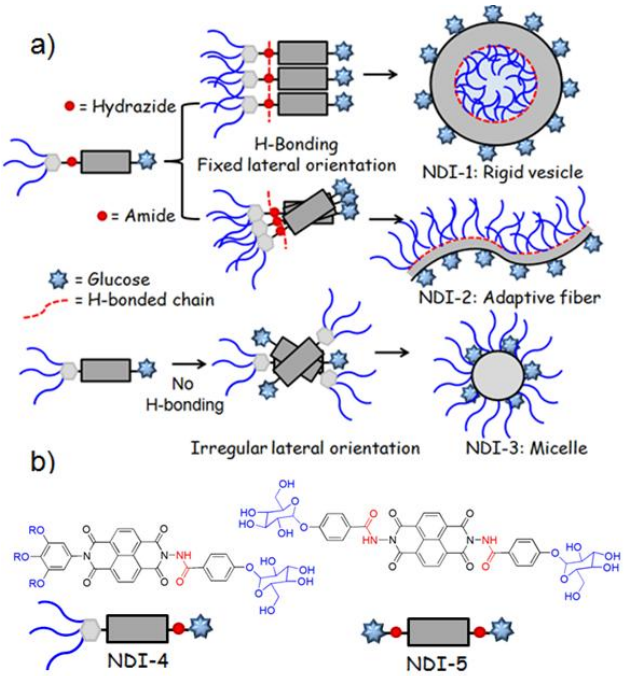


**Scheme 2.** a) Schematic depiction of various nanostructures produced by NDI-amphiphiles. While this scheme shows uni-directional orientation and functional group display and corroborates with the experimental results, in reality some minor deviation cannot be eliminated; b) Structure of the sugar containing control NDI-amphiphiles.

Overall, we have shown that H-bonding can restrict the lateral orientation of the unimers in the assembly of unsymmetric π-amphiphiles and renders an excellent display of ligands. H-bonding also affects the internal order and thus controls the morphology, thermodynamics and adaptability of the resulting nanostructures which strongly impact the multi-valent binding. Cylindrical structure [25] performs better than spherical vesicles. Packing parameter [26] dependent morphology variation and the effect on the multivalent binding and other events have been reported. [27] However, it requires a substantial structural modification and mass change. This communication shows the possibility to achieve the same by a minimal change in the structure as the self-assembly is governed by directional molecular interaction, and thus advocates its enormous potential for precision nanostructures and complex biological function.[28]

## Acknowledgements

AS thanks CSIR, India for a research fellowship. SG thanks DST, India, for funding through the SwarnaJayanti Fellowship Project (DST/SJF/CSA-01/2-14-15).

**Keywords:** Supramolecular assembly • H-bonding • Vesicle • Cylindrical micelle • Multivalent binding

[1] a) D. F. Evans, H. Wennerstrom, *The Colloidal Domain*, 2nd ed.; Wiley-VCH: New York, **1999.**

[2] For reviews on aggregation of amphiphilic polymers see: a) Y. Li, B. S Lokitz; C. L. McCormick, *Angew. Chem. Int. Ed*. **2006**, *45*, 5792; b) T. S. Kale, A. Klaikherd, B. Popere, S. Thayumanavan, *Langmuir* **2009**, *25;* 9660; c) J. Dua, R. K. O'Reilly, *Soft Matter* **2009**, *5*, 3544; d) O. Onaca, R. Enea, D. W. Hughes, W. Meier, *Macromol. Biosci*. **2009**, *9*, 129; e) R. P. Brinkhuis, F. P. J. T. Rutjes, J. C. M. van Hest, *Polym. Chem*. **2011**, *2*, 1449; f) Y. Mai, A. Eisenberg, *Chem. Soc. Rev.* **2012**, *41*, 5969.

[3] a) A. Barnard, D. K. Smith, *Angew. Chem. Int. Ed.* **2012**, *52*, 6572; b) C. Fasting, C. A. Schalley, M. Weber, O. Seitz, S. Hecht, B. Koksch, J. Dernedde, C. Graf, E. W. Knapp, R. Haag, *Angew. Chem. Int. Ed.* **2012**, *51*, 10472.

[4] T. K. Lindhorst, *Top. Curr. Chem.* **2002**, *218*, 201.

[5] a) V. Martos, P. Castreño, J. Valero, J. de Mendoza, *Curr. Opi. In Chem. Bio.* **2008**, *12*, 698; b) B. S. Sandanaraj, D. R. Vutukuri, J. M. Simard, A. Klaikherd, R. Hong, V. M. Rotello, S. Thayumanavan. *J. Am. Chem. Soc.* **2005**, *127*, 10693.

[6] M. A. Kostiainen, J. G. Hardy, D. K. Smith, *Angew. Chem. Int. Ed.* **2005**, *44*, 2556.

[7] S. M. Bromfield, E. Wilde, D. K. Smith, *Chem. Soc. Rev.* **2013**, *42,* 9184.

[8] a) H-J. Kim, T. Kim, M. Lee, *Acc. Chem. Res.* **2011**, *44*, 72; b) S. S. Babu, V. K. Praveen, A. Ajayaghosh, *Chem. Rev.* **2014**, *114*, 1973; c) M.R. Molla, S. Ghosh, *Phys. Chem. Chem. Phys.* **2014**, *16*, 26672; b) c) E. Krieg, M. M. C Bastings, P. Besenius, B. Rybtchinski, *Chem. Rev*. **2016**, *116*, 2414; d) T. Aida, E. W. Meijer, S. I. Stupp, *Science* **2012**, *335*, 813

[9] a) L. Brunsveld, H. Zhang, M. Glasbeek, J. A. J. M. Vekemans, E. W. Meijer, *J. Am. Chem. Soc*. **2000**, *122*, 6175; b) X. Zhang, S. Rehm, M. M. Safont-Sempere, F. Würthner, *Nat. Chem*. **2009**, *1*, 623; c) J. P. Hill, W. Jin, A. Kosaka, T. Fukushima, H. Ichihara, T. Shimomura, K. Ito, T. Hashizume, N. Ishii, T. Aida, *Science* **2004**, *304*, 1481; e) J. F. Hulvat, M. Sofos, K. Tajima, S. I. Stupp, *J. Am. Chem. Soc.* **2005**, *127*, 366; f) N. K. Allampally, A. Florian, M. J. Mayoral, C. Rest, V. Stepanenko, G. Fernàndez, *Chem. Eur. J*. **2014**, *20*, 10669; g) X. Lin, H. Kurata, D. D. Prabhu, M. Yamauchi, T. Ohba, S. Yagai, *Chem. Commun.* **2017**, *53*, 168; h) M. Kumar, S. J. George, *Nanoscale* **2011**, *3*, 2130; i) H. Shao, J. R. Parquette, *Chem. Commun*. **2010**, *46*, 4285; j) M. B. Avinash, E. Verheggen, C. Schmuck, T. Govindaraju, *Angew. Chem. Int. Ed*. **2012**, *51*, 10324; k) S. Ghosh, D. S. Philips, A. Saeki, A. Ajayaghosh, *Adv. Mater*. **2017**, *29*, 1605408; l) J.-H. Ryu, H.-J. Kim, Z. Huang, E. Lee, M. Lee, *Angew. Chem. Int. Ed.* **2006**, *45*, 5304; m) E. Lee, J.-K. Kim, M. Lee, *Angew. Chem. Int. Ed.* **2009**, *48*, 3657; n) G. Na, Y. He, Y. Kim, M. Lee**,** *Soft Matter*, **2016**, *12*, 2846; o) T. Noguchi, B. Roy, D. Yoshihara, J. Sakamoto, T. Yamamoto, S. Shinkai, *Angew. Chem. Int. Ed.* **2016**, *55*, 5708.

[10] a) A. Sikder, A. Das, S. Ghosh, *Angew. Chem. Int. Ed*. **2015**, *54*, 6755; b) A. Sikder, D. Ray, V. K. Aswal, S. Ghosh, *Langmuir* **2018**, *34*, 868.

[11] a) J. J. Lundquist, E. J. Toone, *Chem. Rev.* **2002**, *102*, 555; b) S. R. S. Ting, G. Chen, M. H. Stenzel, *Polym. Chem*. **2010**, *1*, 1392; c) Y. Miura, Y. Hoshino, H. Seto, *Chem. Rev.* **2016**, *116*, 1673.

[12] N. Berger, A. Sachse, J. Bender, R. Schubert, M. Brandl, *Int. J. Pharm*. **2001**, *223*, 55.

[13] E. N. Savariar, S. V. Aathimanikandan, S. Thayumanavan, *J. Am. Chem. Soc.* **2006**, *128*, 16224.

[14] P. Pramanik, D. Ray, V. K. Aswal, S. Ghosh, *Angew. Chem. Int. Ed.* **2017**, *56*, 3516.

[15] M. R. Molla, S. Ghosh, *Chem. Mater.* **2011**, *23*, 95.

[16] D. I. Svergun, M. H. J. Koch, *Rep. Prog. Phys.* **2003**, *66*, 1735

[17] R. Zana, *Langmuir* **1996**, *12*, 1208.

[18] a) J. Kang, J. Rebek, Jr., *Nature* **1996**, *382*, 239; b) C. Schmuck, *Tetrahedron* **2001**, *57*, 3063; c) D. Görl, F. Würthner. *Angew. Chem. Int. Ed.* **2016**, *55*, 12094; d) O. Munkhbat, M. Garzoni, K. R. Raghupathi, G. M. Pavan, S. Thayumanavan, *Langmuir* **2016**, *32*, 2874.

[19] W. Blokzijl, J. B. F. N. Engberts, *Angew. Chem. Int. Ed*. **1993**, *32*, 1545.

[20] a) H. Shi, L. Liu, X. Wang, J. Li, *Polym. Chem.* **2012**, *3*, 1182; b) Y. Miura, T. Ikeda, K. Kobayashi, *Biomacromolecules* **2003**, *4*, 410; c) I. Otsuka, T. Otsuka, H. Nakade, A. Narumi, R. Sakai, T. Satoh, H. Kaga, T. Kakuchi, *Macromolecules* **2007**, *40*, 8930.

[21] T. Furuike, N. Nishi, S. Tokura, S.-I. Nishimura, *Macromolecules* **1995**, *28*, 7241.

[22] F. G. Loontiens, J. P. V. Wauwe, C. K. D. Bruyne, *Carbohydr. Res.* **1975**, *44*, 150.

[23] A. Das, S. Ghosh, *Chem. Commun.* **2016**, *52*, 6860.

[24] F. Würthner, T. E. Kaiser, C. R. Saha-Möller, *Angew. Chem. Int. Ed.* **2011**, *50*, 3376.

[25] a) Y. Geng, P. Dalhaimer, S. Cai, R. Tsai, M. Tewari, T. Minko, D. E. Discher, *Nat. Nanotechnol*. **2007**, *2*, 249; b) X. Wang, G. Guerin, H. Wang, Y. Wang, I. Manners, M. A. Winnik, *Science* **2007**, *317*, 644; c) N. Petzetakis, A. P. Dove, R. K. O'Reilly, *Chem. Sci.* **2011**, *2*, 955.

[26] J. N. Israelachvili, D. J. Mitchell, B. W. Ninham, *J. Chem. Soc., Faraday Trans.* 2 **1976**, *72*, 1525.

[27] a) B.-S. Kim, D.-J Hong, J. Bae, M. Lee, *J. Am. Chem. Soc.* **2005**, *127*, 16333; b) J.-H. Ryu, E. Lee, Y.-B. Lim, M. Lee, *J. Am. Chem. Soc.* **2007**, *129*, 4808; c) D. J. Welsh, P. Posocco, S. Pric, I D. K. Smith, *Org. Biomol. Chem.* **2013**, *11*, 3177; c) Y. Geng, P. Dalhaimer, S. Cai, R. Tsai, M. Tewari, T. Minko, D. E. Discher, *Nat. Nanotechnol.* **2007**, *2*, 249; d) W. Zhao, H. T. Ta, C. Zhang, A. K. Whittaker, *Biomacromolecules* **2017**, *18*, 1145; e) A. C. Rodrigo, S. M. Bromfield, E. Laurini, P. Posocco, S. Pricl, D. K. Smith, *Chem. Commun*. **2017**, *53*, 6335.

[28] M. J. Webber, E. A. Appel, E. W. Meijer, R. Langer, *Nature Mater*. **2016**, *15*, 13.

10.1002/anie.201812217


WILEY-VCH

## Entry for the Table of Contents

# COMMUNICATION

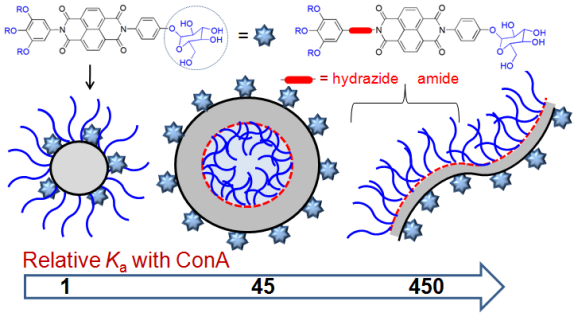


H-bonding regulated lateral orientation and internal order in π-stacked assembly of glucose-appended unsymmetric bola-amphiphiles produces diverse nanostructures with distinct functional group display which makes a strong impact on the multivalent binding efficacy with a biological target.

*Amrita Sikder, Debes Ray, Vinod K Aswal and Suhrit Ghosh**

***Page No. – Page No.***

**Hydrogen Bonding Regulated Supramolecular Nanostructures and Impact on Multivalent Binding**